Available online at www.sciencedirect.com

ScienceDirect

Procedia CIRP 31 (2015) 322 – 327

www.elsevier.com/locate/procedia

15th CIRP Conference on Modelling of Machining Operations

Determination of the Thermal Load Distribution in Internal Traverse Grinding using a Geometric-Kinematic Simulation

S. Schumann[a,*], T. Siebrecht[a], P. Kersting[a,b], D. Biermann[a], R. Holtermann[c], A. Menzel[c,d]

[a]*Institute of Machining Technology, TU Dortmund University, Baroper Straße 303, 44227 Dortmund, Germany*
[b]*Institute of Manufacturing Technology and Quality Management, Otto von Guericke University Magdeburg, Universitätsplatz 2, 30106 Magdeburg, Germany*
[c]*Institute of Mechanics, TU Dortmund University, Leonhard-Euler-Straße-5, 44227 Dortmund, Germany*
[d]*Division of Solid Mechanics, Lund University, P.O. Box 118, 22100 Lund, Sweden*

[*] Corresponding author. Tel.: +49-231-755-5274; fax: +49-231-755-5141. *E-mail address:* schumann@isf.de

Abstract

During grinding processes, numerous grains interact with the workpiece material producing mechanical and thermal loads on the surface. In the field of thermal simulation of grinding processes, a widely used approach is to substitute numerous cutting edges by a single moving distributed heat source of a specific geometrical shape referring to the theory of Carslaw and Jaeger. This heat source is then moved across the modelled workpiece according to the specific kinematics of the grinding process.

The geometrical shape of the substituted heat source can usually be determined using different approaches, e. g., predefined distribution functions or, more precisely, based on measurements of the shear stress within the contact zone. Referring to the state of the art, it is not possible to measure the shear stress within the contact zone during internal traverse grinding with roughing and finishing zone because of its very complex engagement conditions and the non-rectangular shape of its contact zone.

In this work, a novel approach to determining a heat source distribution based on a geometric-kinematic simulation for internal traverse grinding is presented. This simulation identifies the ideal geometrical interaction of workpiece and grinding wheel. For this purpose, the specific material removal rate for each grain is calculated and accumulated with respect to the contact zone resulting in a three-dimensional thermal load distribution. This heat source can be used in finite element simulations to determine the thermal load on the workpiece.

Peer-review under responsibility of the International Scientific Committee of the "15th Conference on Modelling of Machining Operations

Keywords: Grinding; Thermal effects; Geometric modelling; Finite element method (FEM).

1. Introduction

Internal grinding is a machining process with geometrically undefined cutting edges. In contrast to machining processes with a defined cutting edge, material removal is not carried out by a macro-scale tool, but by a large amount of different meso-scale abrasive grains. Internal traverse grinding with a conical roughing zone and a cylindrical finishing zone is a complex machining process resulting in high dimensional, shape, and positional accuracy of the workpiece. Using this process, a high surface quality can be achieved. Prior to the main process, a total stock removal $a_{e,\mathrm{tot}}$ is adjusted (Fig. 1). Afterwards, the rotating grinding wheel generates the inner surface of the rotating workpiece using an axial feed velocity v_{fa}. In this setup, a high material removal rate, which is performed by the conical roughing zone, and a high surface quality, produced by the cylindrical finishing zone, can be achieved in a single grinding stroke [1].

Compared to other grinding processes, internal traverse grinding has a small effective width of the grinding wheel $w_{g,\mathrm{eff}}$ resulting in a high locally concentrated load on the workpiece. This can lead to new hardening or tempered zones, or to thermally induced machining errors, e. g., dimensional failures.

In order to model the thermal load on the workpiece during internal traverse grinding, a simulation framework, which includes three main components at different scales, is being developed [2]. At the meso-scale, a finite element (FE) chip formation model captures the local thermo-mechanical effects on the workpiece surface layer. At the macro-scale, a thermal FE process model according to the theories of Carslaw and Jaeger [3,4] as well as Lowin [5] is used to simulate the global thermal load on the workpiece. To link these two scales, a geometric-kinematic meso-scale simulation is used to represent the engagements of individual grains over time. In this paper, a novel approach to determining a thermal load distribution for the macro-scale FE process model for internal traverse grinding using the geometric-kinematic simulation is presented.

Peer-review under responsibility of the International Scientific Committee of the "15th Conference on Modelling of Machining Operations
doi:10.1016/j.procir.2015.03.020

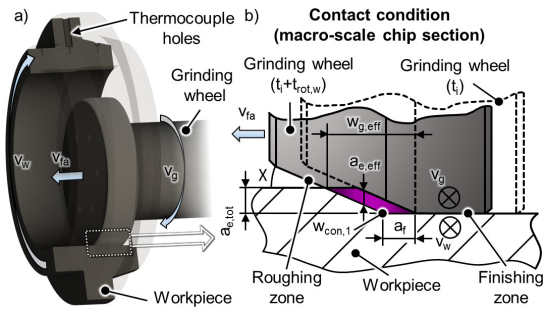

Fig. 1. Internal traverse grinding with two functional zones: a) process kinematics and geometry of the workpiece b) macro-scale chip section with its describing values.

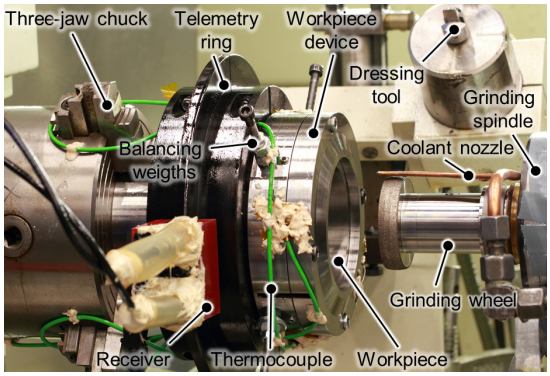

Fig. 2. Experimental setup.

Nomenclature

α	heat transfer coefficient in W/(m^2·K)
τ_t, σ_n	shear and normal stress in N/mm
χ	roughing zone angle in °
$a_{e,\mathrm{tot}}$	total radial stock removal in mm
$a_{\mathrm{ed,tot}}$	total radial dressing stock removal in µm
$a_{e,\mathrm{eff}}$	effective depth of cut in mm
a_f	axial feed in mm
d_s	diameter of workpiece in mm
d_w	diameter of grinding wheel in mm
F_t, F_n	tangential and normal force in N
F'_t, F'_n	specific tangential and normal force in N/mm
l_c, l_g	contact length, geometric contact length in mm
l_{con}	FE grid division in x-direction in mm
l_e	length of one element in FE grid in mm
n_g	grinding wheel rotational speed in min^{-1}
n_w	workpiece rotational speed in min^{-1}
$\dot{q}$	heat flux in W/m^2
t	time in s
T	temperature in °C
t_{rot}	time per revolution in s
v_{fa}	axial feed velocity in mm/min
v_g	grinding wheel velocity in m/s
v_w	workpiece velocity in m/s
V_w	material removal in mm^3
w_{con}	FE grid division in y-direction in mm
w_g	width of grinding wheel in mm
$w_{g,\mathrm{eff}}$	effective width of grinding wheel in mm
Q_w	material removal rate in mm^3/s
Q'_w	specific material removal rate in mm^3/(mm · s)
Q''_w	specific material removal rate in mm^3/(mm^2 · s)

2. Experimental setup

Forces and temperatures during internal traverse grinding have to be known for determining local values within the contact zone, e. g., shear stresses or heat fluxes, and to calibrate the heat input of the macro-scale FE model. Hence, high-speed grinding experiments (v_g = 120 m/s) were carried out with an internal grinding machine (type IC 400 by Overbeck). The workpiece is axially clamped in a device which is attached in a three-jaw chuck (Fig. 2). To measure the temperature below the contact zone during the grinding process, type K thermocouples (∅ = 0.25 mm) are positioned in external holes within the workpiece (cf. Fig. 1a). These are connected with a three-channel telemetry ring by the company Manner which is externally mounted to the device. Measured data of the rotating workpiece system is transferred to the measurement equipment. The grinding wheel is mounted in a HSK grinding spindle. The spindle is attached to a force dynamometer (type 9255B by Kistler). In order to ensure stable process conditions, both, grinding wheel and workpiece device, were precisely balanced in the machine before carrying out the experiments. An electroplated single-layered CBN grinding wheel was used during the experiments. The nickel-based bonding allows a high-strength loading of the grains and, thus, the application of high material removal rates. The topography comprises dominant grains with large protrusion heights resulting in pattern formation on the surface of the workpiece [1]. To represent industrial machining conditions and to improve the surface quality, the grinding wheel was touch dressed with a single diamond grain with a total radial dressing stock removal $a_{\mathrm{ed,tot}}$ = 16 µm according to [1]. The cooling during machining was realised by a coolant supply via a bi-functional nozzle. On the one hand, small holes in the nozzle are oriented radially towards the grinding wheel in order to remove adhesive chips. On the other hand, a larger hole in the nozzle is oriented towards the process zone to reduce the friction and to ensure sufficient cooling during the process. In Table 1 additional experimental boundary conditions are shown.

To model the meso-scale grinding wheel, the distributions

Table 1. Experimental boundary conditions

Description	Value
Grinding wheel velocity	v_g = 120 m/s
Workpiece velocity	v_w = 2 m/s
Axial feed	a_f = 0.25 ... 0.75 mm
Total radial stock removal	$a_{e,\mathrm{tot}}$ = 0.15 mm
Workpiece material	102Cr6 hardened to 62-64 HRC
Roughing zone angle	χ = 7.5°
Width of roughing zone	w_r = 4 mm
Width of finishing zone	w_f = 4 mm
Process strategy	down grinding

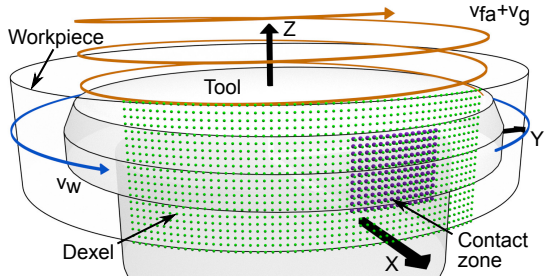

Fig. 3. Dexel-based modelling of the internal traverse grinding process. The blue arrow represents the rotation of the workpiece and the orange arrow is the trajectory of a grain on the tool.

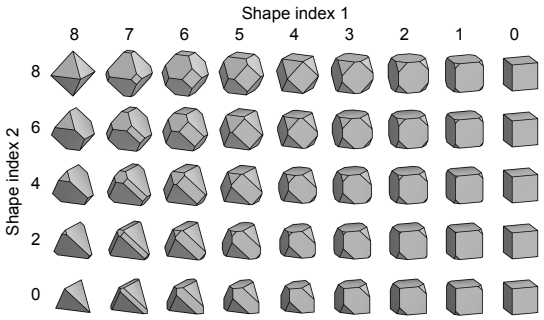

Fig. 4. CSG shapes of CBN cutting grains (cf. [13]).

of the diameters and protrusion heights of the grains are required. The sizes of approximately 1500 grains were measured with a light microscope (type VHX-500F by Keyence). The grinding wheel topography was measured using replica material and a structured light microscope (type GFM MikroCAD by GFMesstechnik GmbH). Afterwards, a topography analysis was performed [6]. Representative distributions of the protrusion heights and grain diameters, and the number of relevant grains per surface area of the grinding wheel were estimated and implemented in the geometric-kinematic simulation.

3. Geometric-kinematic simulation

Grinding processes can be modelled using different approaches like, e. g., FE analysis [7] or particle-based simulations [8]. Geometric-kinematic approaches allow a time-domain simulation of grinding processes based on the movement of the grinding wheel and the shape of the contact situation [7]. In order to calculate these geometric contact situations during grinding processes, the shape of the workpiece and the grinding tool have to be modelled. To represent the shape of the workpiece, dexel-based approaches like multidexel boards [9] or poisson-disk-sampled dexel distributions [10] have been applied successfully. Due to the cylindrical shape of the workpieces in internal grinding processes, a cylindrical heightfield is used in the presented work. Assuming that the process behaviour is equal in different radial sections of the workpiece, it only has to be modelled partially as shown in Fig. 3. In each cell of the heightfield, the local radius, which is initially set to the inner radius of the workpiece, is stored. In this way, material removal, which is assumed to be ideal, can be modelled by increasing these radius values.

The grinding tools can be modelled using different approaches as well. If only the macroscopic engagement situation is of interest, the shape of the tools can be represented using the constructive solid geometry (CSG) technique [11]. Considering the meso-scale influence of the individual cutting grains, e. g., surface topographies or process forces per grain can be modelled [12]. Using the CSG technique, the ideal shape of diamond or CBN grains can be modelled as the intersection of a hexahedron, an octahedron and a tetrahedron [10,13]. By scaling these primitives appropriately, different shapes can be generated. Several simulated grain shapes, which can be identified using a pair of index values, are shown in Fig. 4. The grains are distributed randomly on the surface of the grinding tools based on normal distributions of the diameter and the shape index, and a gamma distribution of the protrusion height. The internal grinding process is simulated by moving and rotating the grinding tool and the workpiece in fixed time steps according to the given process parameters. These parameters include the axial feed velocity v_{fa}, the velocity of the workpiece v_w and the tool v_g, and the total radial stock removal $a_{e,\mathrm{tot}}$. In order to model the touch dressing of the grinding wheel, the CSG model of the tool is extended by an additional cylinder with the dressing diameter mentioned in chapter 2. The radius of the grinding grains is reduced by intersecting their shape with this dressing cylinder. The chip shapes are calculated as the intersections between each numerically touch-dressed grain on the grinding tool and the workpiece material. This intersection is removed from the workpiece in order to model an ideal cutting process.

For the formulation of the FE thermal load distribution, the material removal within the classical contact zone in grinding according to [14] have to be known. Thus, in the used simulation setup, a contact zone grid is defined (Fig. 3). This grid is moved with the grinding wheel in axial direction without rotating. In every simulation step, the volume of the removed material is transferred from the heightfield to the contact zone grid. After each revolution of the grinding wheel, the state of the contact grid is stored and the values of the grid cells are reset to their initial state. For further calculations, only the material removal during the steady state grinding process is used (cf. section 5).

4. Macro-scale thermal FE model for internal traverse grinding

The approach of Carslaw and Jaeger [3,4] is widely used in thermal FEA. Every single grain load is included in a macro-scale heat source which induces a heat input into the workpiece along the contact zone. This heat source is moved over the modelled workpiece according to the process kinematics. Lowin extends this approach with convective boundary conditions to represent the coolant and its effect during the grinding process [5]. In internal traverse grinding, a very high calculation time is necessary to model the workpiece ensuring an adequate discretisation. Therefore, only a macro-scale model of a reference volume segment of the workpiece was developed in ANSYS. This segment is limited by the width of the workpiece in axial direction and the contact length l_c in circumferential direction. When the grinding wheel is in contact with the reference segment, a load step is applied (Fig. 5).

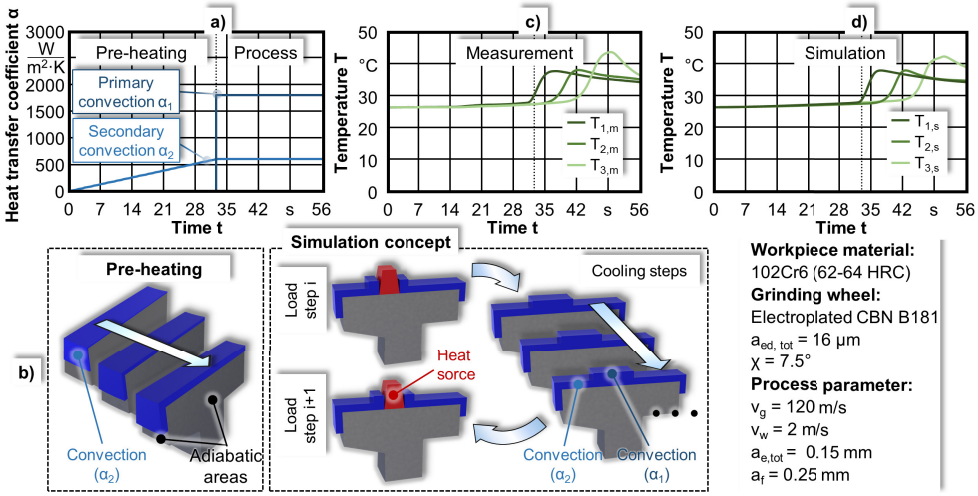

Fig. 5. Macro-scale FE model with implemented pre-heating capturing the global thermal load on the workpiece during internal traverse grinding: a) heat transfer coefficients over simulation time, b) simulation concept, c) measured thermocouple temperatures below the contact zone, d) simulated temperatures at the thermocouple position, which are used to calibrate the FE simulation.

Afterwards, cooling steps are performed before applying the next load step, in which the heat source is axially shifted by the axial feed a_f. To represent the coolant in the model, two-stage convective boundary conditions are used. During the process, the coolant nozzle is oriented towards the contact zone. This results in a stronger convective effect expressed in a higher primary heat transfer coefficient in this section of the model. Due to the high rotational speed of the grinding wheel, the fluid is spread in the whole working space. Hence, secondary convective boundary conditions are applied with a smaller heat transfer coefficient (Fig. 5). The temperature of the coolant was measured during the experiments and is used as the second input for both convective boundary conditions.

Due to the higher temperature of the coolant, prior to the process, the workpiece is pre-heated while the rotating grinding wheel approaches. To model this, a pre-heating phase is implemented in which only a rising secondary convection is applied (Fig. 5). The material data for the thermal model is shown in Table 2.

5. Formulation of the FE heat source distribution based on the local specific material removal rate

According to the process power theory of Lowin [5], uniformly distributed heat flux in grinding processes within the contact zone can be calculated by equation (1). The process power is related to the area of the contact zone A_{con}. In this equation, the heat transformation factor K_v describes the mechanical power which is transformed into thermal energy. The heat distribution factor K_w takes the heat input into the workpiece into account. In the presented work, the heat transformation factor is $K_v = 1$ and the heat distribution factor is adapted by an iterative matching between measured and simulated temperature.

Table 2. Material data (cf. [5])

Description	Value
Specific heat capacity	c_p = 480 W/(kg·K)
Thermal conductivity	λ = 21.07 W/(m·K)
Density	ρ = 7830 kg/m^3

$$\dot{q} = \frac{F_t \cdot v_g \cdot K_w \cdot K_v}{l_c \cdot w_{g,\mathrm{eff}}} \;\wedge\; l_c = l_g \tag{1}$$

The shape of the heat source is usually based on predefined distribution functions, e. g., triangular or rectangular distributions (cf. [7]). In surface grinding with its simple rectangular form of the contact zone, it is possible to use the shear stress to estimate the shape of the heat source [15] (cf. equation (2) and (3)).

$$\dot{q}\,(w_{\mathrm{con}}, l_{\mathrm{con}}) = \tau_t\,(w_{\mathrm{con}}, l_{\mathrm{con}}) \cdot v_g \cdot K_w \cdot K_v \tag{2}$$

$$\dot{q}\,(w_{\mathrm{con}}) = \frac{F_t'\,(w_{\mathrm{con}}) \cdot v_g \cdot K_w \cdot K_v}{l_c} \;\wedge\; l_c = l_g \tag{3}$$

These formulations are based on measurements of the mentioned specific values according to the works of Shafto and Noyen in surface grinding [15,16]. Furthermore, the shape of the heat source can be determined using weighting functions referenced to the macro-scale approach of the chip section. Therefore, the average of the tangential force is redistributed by the specific removal rate Q_w' along the effective width of the grinding wheel $w_{g,\mathrm{eff}}$ [17] (cf. equation (4)).

$$\dot{q}\,(w_{\mathrm{con}}) = \frac{F_t'\,(Q_w'\,(w_{\mathrm{con}})) \cdot v_g \cdot K_w \cdot K_v}{l_c} \;\wedge\; l_c = l_g \tag{4}$$

In this paper, the contact zone grid of the geometric-kinematic simulation is used to calculate the material removal in the contact zone (Fig. 6a). In the first step, the material removal is mapped to the FE discretisation. For this purpose, the sum of the material removal is calculated in the discretisation grid of the macro-scale FE model (Fig. 6b). To estimate the specific area with respect to the material removal rate related to one revolution of

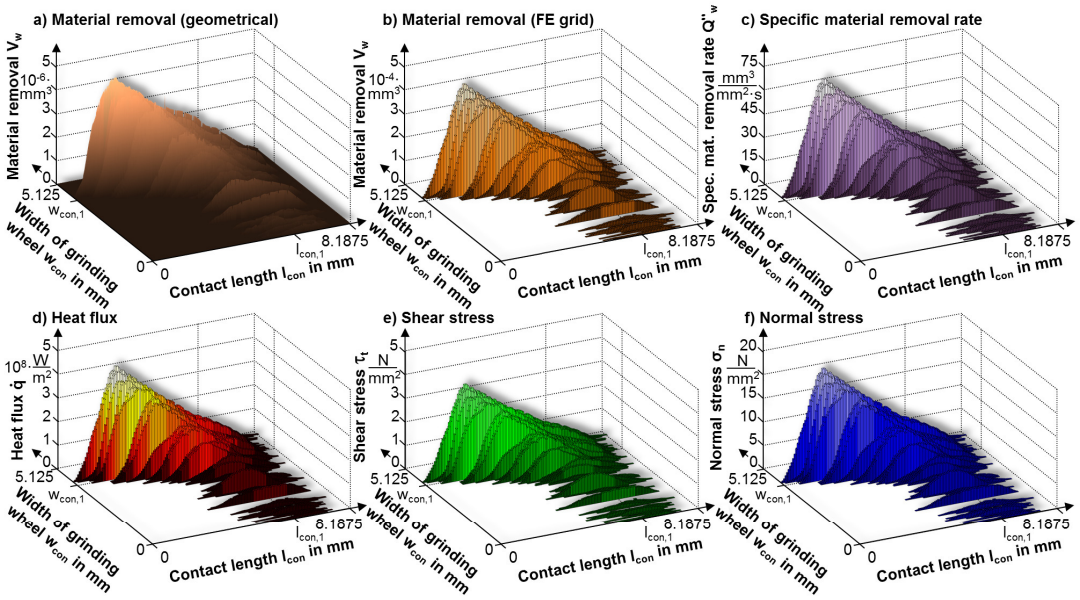

Fig. 6. Calculated representative values within the contact zone during internal traverse grinding (a_f = 0.75 mm, $a_{e,\mathrm{tot}}$ = 0.15 mm). l_{con} = 0 mm represents the beginning of possible grain material removal and $l_{\mathrm{con,max}}$ = 8.1875 mm is the end of possible grain material removal along the contact length l_c. The value $l_{con,1}$ is the end of the macro-scale contact zone. In direction of the width of the grinding wheel, w_{con} = 0 mm represents the beginning of the finishing zone, $w_{\mathrm{con},1}$ is the transition between the roughing and finishing zone (cf. Fig. 1), and $w_{\mathrm{con,max}}$ = 5.125 mm is the end of the grinding wheel engagement in axial direction. The calculated values are based on results of the geometric-kinematic simulation and force measurements, considering the contact zone formulation for one revolution of the grinding wheel: a) raw data of the material removal within the contact zone (resolution = 0.00625 mm), b) material removal within the contact zone considering the FE model discretisation (resolution = 0.0625 mm), c) specific material removal rate within the contact zone, d) heat flux within the contact zone with K_w = 1, e) shear stress within the contact zone, f) normal stress within the contact zone.

the grinding wheel, equation (5) is used (Fig. 6c). In the next step, the average tangential and normal forces are redistributed while keeping the specific removal rate constant (Fig. 6e and Fig. 6f). In this context, the specific removal rate is assumed to be proportional to the process forces. Afterwards, the discrete heat flux in the FE grid is calculated according to equation (6) (Fig. 6d).

$$Q''_w(w_{\mathrm{con}}, l_{\mathrm{con}}) = \frac{V_w(w_{\mathrm{con}}, l_{\mathrm{con}})}{{l_e}^2 \cdot t_{\mathrm{rot},g}} \tag{5}$$

$$\dot{q}(w_{\mathrm{con}}, l_{\mathrm{con}}) = \tau_t\left(Q''_w(w_{\mathrm{con}}, l_{\mathrm{con}})\right) \cdot v_g \cdot K_w \cdot K_v \tag{6}$$

In the macro-scale FE model, the heat input is applied in one single load step per overrun of the heat source. Hence, the thermal load distribution has to be transformed to the boundary conditions of the model. Numerical integration of the heat flux along the contact length is used and related to the maximum contact length $l_{\mathrm{con,max}}$ resulting in a uniform distribution of heat flux along the contact length (cf. equation (7)).

$$\dot{q}(w_{\mathrm{con}}) = \sum_{j=l_{\mathrm{con,first}}}^{l_{\mathrm{con,last}}} \dot{q}(w_{\mathrm{con}}, j) \cdot \frac{l_e}{l_{\mathrm{con,max}}} \tag{7}$$

Using the procedure shown in Fig. 7 under consideration of equation (7), simulations were conducted to determine the global thermal load during internal traverse grinding. The comparison between measured and simulated temperatures below the contact zone are shown in Fig. 5c and Fig. 5d.

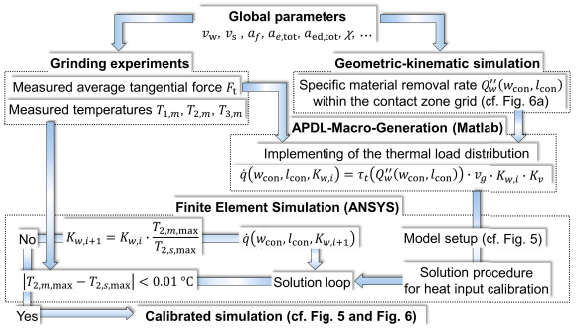

Fig. 7. Simulation framework: Based on the global process parameters, the grinding experiments and the geometric-kinematic simulations are conducted. The local heat flux is calculated according to the modified process power theory of Lowin (cf. Fig. 6). By matching the maximum measured and simulated temperatures iteratively, the simulation is calibrated.

6. Results and Discussion

Using the presented approach, calibrated simulations of two processes with different axial feeds are compared (Fig. 8). A higher axial feed results in a higher thermal load on the workpiece in this process parameter space. In addition to the thermal state, the global mechanical load on the workpiece rises as well: $F_{t,a_f,0.25}$ = 5.80 N, $F_{n,a_f,0.25}$ = 22.64 N; $F_{t,a_f,0.75}$ = 11.93 N, $F_{n,a_f,0.75}$ = 56.32 N. From a macro-scale technological point of

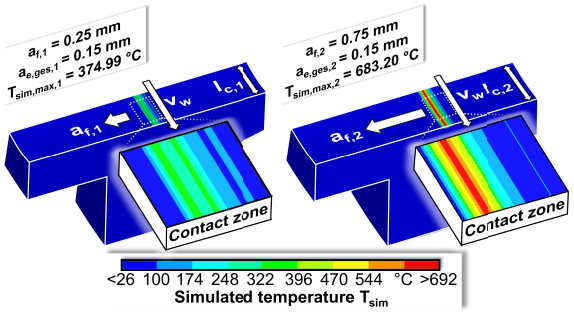

Fig. 8. Simulated thermal load on the workpiece of two different internal traverse grinding processes varying axial feed.

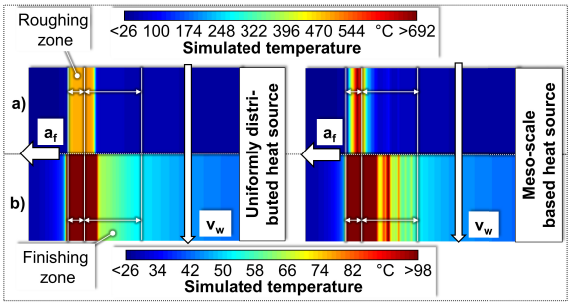

Fig. 9. Comparison between simulated temperatures within the contact zone which were obtained using a classical uniformly distributed heat source according to the chip section and the novel meso-scale based heat source in the presented FE model (a_f = 0.75 mm, $a_{e,ges}$ = 0.15 mm): a) results with full temperature range, b) results with temperatures between 26 °C and 98 °C.

view, the global removal rate is three times higher using the larger axial feed: $Q_{w,a_f,0.25}$ = 75 mm^3/s, $Q_{w,a_f,0.75}$ = 225 mm^3/s. At the meso-scale, this means that the individual grains have to remove a larger amount of material. Regarding the topography of the grinding wheel, lower-lying grains participate in the material removal process, which results in a higher amount of active grains.

To compare calibrated simulation results using a classical uniform thermal load distribution and the meso-scale approach, the temperatures within the contact zone are shown in Fig. 9. Considering local grain engagements by the heat source, temperature peaks occur within the contact zone (cf. Fig. 9b right). Using the uniform thermal load distribution, the maximum temperatures are smaller.

7. Conclusion and Outlook

In this paper, a novel approach for modelling a thermal heat distribution based on the average measured process forces and the specific removal rate is introduced. In this context, a meso-scale geometric-kinematic simulation is combined with a macro-scale FE model for internal traverse grinding. In comparison to the classical approach, the meso-scale simulated temperature peaks occur within the contact zone because of locally concentrated grain engagements. In order to consider meso-scale effects, e. g., decreasing specific forces with higher single grain chip thickness, in the formulation of the presented thermal load distribution, process force models [12,18] or meso-scale FE chip formation models [2] should be used.

Acknowledgements

Financial support by the German Research Foundation (DFG) in the context of SPP 1480 (project IDs: ME 1745/7-3; BI 498/23-3) is gratefully acknowledged.

References

[1] Marschalkowski K, Biermann D, Weinert, K. On the characteristics of high-performance internal peel grinding using electroplated CBN wheels. Machining Science and Technology, 2012:16:4, p. 580-600.
[2] Holtermann R, Schumann S, Menzel A, Biermann D. A Hybrid Approach to the Modelling and Simulation of Grinding Processes. In: Proceedings of 11th. World Congress Computational Mechanics (WCCM XI) - Ebook Volume III World Congress, Barcelona, Spain, 2014, p. 1932-1937.
[3] Carslaw HS, Jaeger JC. Conduction of Heat in Solids. London: Oxford University Press; 1959.
[4] Carslaw HS, Jaeger JC. Moving Sources of Heat and the Temperature at Sliding Contacts. In: Journal and Proceeding of the Royal Society of New South Wales 1942;76:3. p. 203-224.
[5] Lowin R. Schleiftemperaturen und ihre Auswirkungen im Werkstück. Dissertation Aachen; 1980.
[6] Holtermann R, Schumann S, Menzel A, Biermann D. Modelling, simulation and experimental investigation of chip formation in internal traverse grinding. Production Engineering - Research and Development 2013;7:2-3, p. 251-263.
[7] Brinksmeier E, Aurich JC, Govekar E, Hoffmeister HW, Klocke F, Peters J, Rentsch R, Stephenson DJ, Uhlmann E, Weinert K, Wittmann M. Advances in modeling and simulation of grinding processes. In: CIRP Annals Manufacturing Technology Bd. 2006;55:2, p. 667-696.
[8] Ruttimann, N ,Buhl S, Wegener K. Simulation of single grain cutting using sPH method. In: Journal of Machine Engineering 2010;10:3, p. 17-29.
[9] Mohn T, Rausch S, Biermann D. Grinding simulation by technologically enhanced and geometrically optimized multidexel models. In: Proc. of 7th CIRP international conference on intelligent computation in manufacturing engineering (ICME), Capri (Gulf of Naples), Italy; 2010, digital published.
[10] Siebrecht T, Rausch S, Kersting P, Biermann, D. Grinding process simulation of free-formed wC-co hard material coated surfaces on machining centers using poisson-disk sampled dexel representations. In: CIRP Journal of Manufacturing Science and Technology, 2014;7.
[11] Foley JD, Van Dam A, Feiner SK, Hughes JF, Phillips RL. Introduction to computer graphics. 1st ed. Boston: Addison-Wesley Longman Publishing Co.; 1994.
[12] Aurich JC, Kirsch B. Kinematic simulation of high-performance grinding for analysis of chip parameters of single grains. In: CIRP Journal of Manufacturing Science and Technology 2012:5, p. 164-174.
[13] Jackson, MJ, Davim JP. Machining with Abrasives. 1st edition Berlin Heidelberg: Springer-Verlag; 2011.
[14] Klocke, F. Manufacturing Processes 2 – Grinding, Honing, Lapping. Berlin Heidelberg. 1st edition Berlin Heidelberg: Springer-Verlag; 2009.
[15] Weinert K, Noyen, M. Analysis and Simulation of the Thermomechanical Load on the Workpiece in the Grinding Process. In: Proceedings of the 2nd Manufacturing Engineering Society, International Conference, CISIF-MESIC 2007, Madrid, Spain; 2007, digital published.
[16] Shafto GR. Creep Feed Grinding An investigation of surface grinding with high depths of cut and low feed rates. Dissertation Bristol; 1974.
[17] Schumann S, Holtermann R, Biermann D, Menzel A. Hochleistungs-Innenrundschälschleifen - Thermomechanische Betrachtung in Abhängigkeit vom radialen Gesamtaufmass. diamond business. 2013;11:2, p. 36-43.
[18] Kienzle O, Victor H. Die Bestimmung von Kräften und Leistungen an spanenden Werkzeugen und Werkzeugmaschinen. VDI-Z 1952;94; p.299-305.